How to Cite:
Nivethitha, A., Baskar, D., Murali, L., & Anandaselvakarthik, T. (2022). Deep clustering with convolution autoencoders and edge detection based classifcation and visualization of Alzheimer's disease. *International Journal of Health Sciences*, *6*(S2), 10288–10302. https://doi.org/10.53730/ijhs.v6nS2.7751

Deep clustering with convolution autoencoders and edge detection based classifcation and visualization of Alzheimer's disease

Ms. A. Nivethitha
PG Scholar, Hindusthan College of Engineering & Technology
Corresponding author email: nivearjun14@gmail.com

Dr. D. Baskar
Associate Professor, Hindusthan College of Engineering & Technology
Email: baskardr@gmail.com

Dr. L. Murali
Associate Professor, P. A. College of Engineering & Technology
Email: murlak37@gmail.com

Mr. T. Anandaselvakarthik
Assistant Professor, Hindusthan College of Engineering & Technology
Email: tanandskarthik@gmail.com

***Abstract*---**Although there is no treatment for ADs (Alzheimer's Diseases), accurate and early diagnosis is critical for both patients and caregivers, and it will become much more vital if disease-modifying medicines are available to prevent, cure, or even halt the illness's course. One of the most active study topics in the medical industry in recent years has been the categorization of ADS using deep learning algorithms. However, most existing approaches are unable to utilise all spatial information, and so lose inter-slice correlation. To avoid this issues in recent works introduces CAEs (convolution auto encoders) based unsupervised learning for classifying ADs from NCs (normal controls), and supervised transfer learning is applied to solve classifications of Ads into pMCIs (progressive mild cognitive impairments) and sMCIs (stable mild cognitive impairments). A gradient-based visualisation technique that approximates the geographical effect of CNNs (Convolution Neural Networks) decisions were used to determine the most relevant biomarkers connected to ADs and pCMIs. Despite the fact that DLTs (deep learning techniques) perform well, finding optimal performing network structures for certain applications is not easy since it is frequently unclear how network structure affects network accuracies.

This can be solved through hyper parameter tuning of DLTs. To mitigate the above mentioned problems in this work first introduced a pre-processing step using median filtering to remove the unwanted noises in images. Subsequently, Canny edge detection operators are used to carry out edge detections. These techniques in image processing locate boundaries of image objects in analysis. To achieve a large border separation, the system looks for variations and discontinuities in the brightness of neighbouring pixels. The picture is also sent into Deep Clustering using CAEs for classification of ADs and NCs. Experimental results exhibit proposed model's effectiveness in terms of precisions, recalls, accuracies and f-measures.

***Keywords*---**Alzheimer's disease, median filtering, supervised transfer learning.

Introduction

Ads are gradual and degenerative brain illnesses that affect millions of individuals throughout the world. According to the World Health Organization's 2019 report, counts of people affected with ADs in America is a predicted 5.8 million, with the possibility of this number rising to 13.8 million by mid-century. Atrophy or shrinking of the brain, which happens owing to the slow degradation of nerve cells, is one of the key alterations in the brain linked with ADs. This shift is considered to have started 13 years before cognitive symptoms like memory loss and other behavioural abnormalities appeared. Because of its outstanding spatial resolution, enhanced accessibility, high contrast, and lack of radiation in the scanning procedure, MRI (Magnetic resonance imaging), a non-invasive approach is used to examine brain atrophy changes and has been frequently employed in studies on ADs [1].

Despite extensive investigation, there is no definitive diagnosis in modern clinical practise due to identical and overlapping symptoms. Only after the patient's death can the presence of ADs be definitively established by a post mortem study of brain tissues making it imperative to detect ADs early for patients and much more crucial when medicines to arrest the disease's development become available. Many hand-crafted machine learning algorithms have accurately identified ADs early where their categorizations, these approaches extract user-defined discriminating characteristics from brain imaging data [2,3].

According to the study, machine learning-based approaches can predict ADs significantly more accurately than radiologists. However, without domain knowledge, defining traits that completely differentiate each class is always challenging. DLTs have recently become popular for categorizations of ADs where they extract hidden features from measurements of ROIs (Regions of interest) of various brain imaging data. However, approaches based on ROIs are unable to take use of all geographical data. Although these approaches lower the size of the characteristics greatly, they may miss certain minor aberrant alterations. Deep CNNs can help solve this issue [4,5].

Recent research uses CAEs-based unsupervised learning to distinguish ADs from NCs, and supervised transfer learning to distinguish pCMIs from sMCIs. Visualized gradients approximated CNN's geographical effects for decisions on ADs and pMCIs related biomarkers. Despite the fact that DLTs perform well in finding the optimal performing network structures for certain applications which is not easy since it is frequently unclear how network structure affects network accuracies which can be solved by hyper parameter tuning of DLTs.

To mitigate the above mentioned problems in this work first introduced a pre-processing step using median filtering to remove the unwanted noise in the image. And then edge detection is proposed using canny edge detection operator. Edge detections locate and detect boundaries of image objects during analysis. Systems examine variations and discontinuities in pixel brightnesses for significant boundary separations. Further the image is fed into the Deep Clustering with CAEs for classifying ADs and NCs .

Literature Review

Zhang et al [2017] [6] proposed feature extractions based on landmarks for detecting ADs from longitudinal structural MRI images as they do not need non-linear registrations or tissue segmentations while being robust to differences in longitudinal scans. The study distinctively found 1) discriminative landmarks automatically from brain images in training and localised landmark detections on test images, without using nonlinear registrations or tissue segmentations; 2) high-level statistics of spatial and contextual longitudinal features were extracted based on detected landmarks, thus characterizing spatio-structural properties; and 3) absorptions. Linear SVMs (support vector machines) differentiate people with Ads or minor cognitive deficits from healthy controls using spatial and longitudinal data. Classification accuracies of 88.30% for Ads or mild impairments and 79.02% for healthy individuals in experimental findings on the ADNI (Alzheimer's Disease Neuroimaging Initiative) database indicate the proposed method's improved performance and efficiency.

To learn the different characteristics from MR brain pictures, Li,et al [2017][7] proposed a classification technique based on a mixture of multimodel 3DCNNs. The MR picture is first hierarchically transformed into more compact high-level features using a deep 3DCNNs. Second, characteristics from MRI brain images are extracted using multiscale 3DCAEs (3D CAEs). For picture classification in ADs diagnosis, the characteristics gained by these models are integrated with the top fully linked layers. Without segmenting brain tissues and regions, the suggested technique may automatically learn general characteristics from imaging data for categorization. T1-weighted MRI brain scans of 428 people, comprising 199 AD patients and 229 NCs from the ADNI database, were used to test the study's technique. The suggested technique obtains an accuracy of 88.31 percent for ADs classification and an AUC of 92.73 percent for AUCs (area under the ROC curves), indicating good classification capabilities.

CNNs were used to identify ADs and moderate impairments by Billones et al [2016] [8]. On the ADNI dataset, the study updated the 16-layered VGGNet for 3-way classification of ADs and mild impairments from healthy people. The study

achieved 91.85% accuracy and out beating other classifiers in bechmarks. Wang,et al [2018][9] proposed using CNNs for multi-modal analyses of MRIs that could also be used to analyse single type MRI data. First, from multimodal MRI data, the human brain network connectivity matrix was generated and utilised as the input data for CNNs. Then, to analyse the network matrix and categorise ADs, aMCIs (amnestic mild cognitive impairments) patients, and NCs, a unique CNNs framework was presented. The benefit of this technique is that it uses a CNN's convolution kernel to mix multimodal MRI data and produce a greater classification accuracy. When utilising multimodal MRI data as inputs, ADs, aMCIs, and NCs were classified with an accuracy of 92.06% for multimodal MRIs. Unique DLTs were used by Feng et al [2019] [10]. Our architecture takes advantage of the benefits of 3DCNNs and FSBi-LSTMs (fully stacked bidirectional long short-term memory). The study's 3DCNNs extracted in-depth feature representations from MRIs and PETs images. Their use of FSBi-LSTMs on hidden spatial information from deep feature maps enhanced final performances. Finally, we use the ADNI dataset to test our technique. For distinguishing ADs from NCs, pMCIs from NCs, and sCMIs from NCs, our technique obtains average accuracies of 94.82 percent, 86.36 percent, and 65.35 percent, respectively, and surpasses the related algorithms.

Hosseini-Asl, et al. [2016] [11] suggested deep 3DCNNs for predicting ADs as they have the capability to learn generic features and capture biomarkers for ADs in multiple datasets. The 3DCNNs are based on 3DCAEs that previously learn shape differences in anatomical structures of the brain from MRIs. The study fine-tuned fully linked higher layers of 3DCNNs for categorizing ADs. Experiments on the CADDementia MRI dataset without any pre-processing revealed that 3DCNNs beats various traditional classifiers in terms of accuracy. The ADNI dataset was used to validate the 3D ability of CNNs to generalise and adapt learned features to various domains.

Manzak,et al [2019][12] intended to develop a rapid and accurate automated classification method for determining ADs using the least amount of patient data possible. MRIs are commonly used to diagnose ADs. Different solutions are required when the expense of the technology and the dangers of the operations were evaluated for detections of ADs with portable devices. Using DNNs (Deep Neural Networks), the study offered a quick and effective technique for detecting ADs. RFs (Random Forests) deleted some characteristics in order to lower the algorithm's complexity. The success of RFs in eliminating features and DNNs in detecting ADs was addressed.

Proposed methodology

This section discuss the proposed ADs classification in detail. Proposed model consist of four phases. First one is pre-processing using median filtering based noise removal, second one is edge detection using canny edge detection operator, third one is Deep Clustering with CAEs based ADs and NCs. Overall architecture of the proposed model is shown in figure: 1.

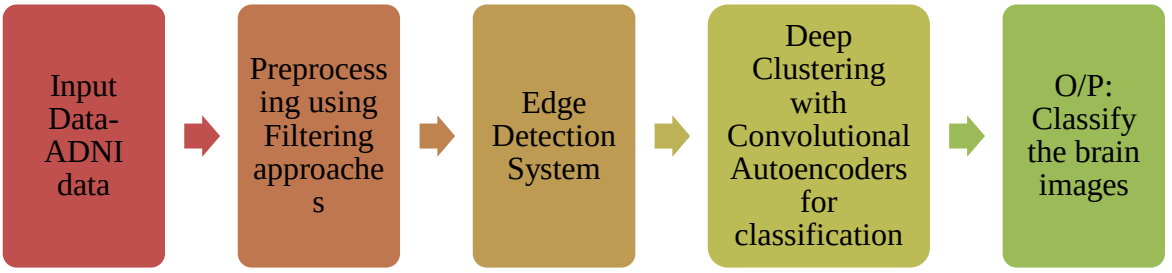

Figure: 1.Overall architecture of the proposed model

Input

Use the ADNI dataset in this project, which is freely available on the internet (http://adni.loni.usc.edu/). The ADNI intends to find more sensitive and accurate methods for detecting ADs early on, as well as biomarkers to track the progression of the disease. In this study, 694 structural MRI images were utilised, with ADs (n = 198), NCs (n = 230), pMCIs (n = 166), and sCMIs (n = 101) being the initial classifications. The 166 pMCIs individuals were initially diagnosed with MCI, but after a 36-month follow-up, they were found to have converted to ADs. The participants were aged 55 to 90, and the MMSE scores for each group were 20–26 (ADs), 24–30 (MCI), and 24–30 (NCs). CDRs (clinical dementia ratings) were 0 for NCs participants, 0.5 for moderate impairment subjects with an obligatory memory box score of at least 0.5, and 0.5 or 1 for ADs individuals. Because sMCIs are a single modality, most of the available sMCIs scans in the ADNI database were included, with the exception of scans of unexplained MCI (n = 130), in which the participants were missing a diagnosis 36 months after baseline.

Pre-processing using median filtering

The filter is non-linear. It performs much better than the mean filter. The median value of all pixels replaces the centre pixel, resulting in reduced blurring. It is utilised to minimise impulsive speckle noise because of its nature [13,14,15]. It has the advantage of preserving the edges.

1. Draw a 3 3 (or 55, or whatever) area around the pixel (i, j).
2. Sort the pixels in the region's intensity values in ascending order.
3. Change the pixel value to the midway value (i, j).

Edge detection using canny edge detection operator

The borders of brain pictures must be identified before objects can be identified. Canny operators improve single threshold approaches by selecting higher and lower limits for thresholds based on histogram gradients of images. All edge

detection techniques have the same goal that of finding edges without any prior knowledge. The five main stages of canny edge detections are smoothing, filtering, finding gradient magnitudes and directions, suppressing non-maxima, dual thresholds, and tracing the edges using hysteresis [16,17,18].

Various Gaussian kernels can smooth the picture. After smoothing, the Canny edge detections locate edges with higher variations in grey level intensities where image gradients find these locations. Sobel operators determine gradients of pixels where initial estimations consider directions x and y of the gradients using the kernels below:

$$K(G_x) = \begin{pmatrix} -1 & 0 & 1 \\ -2 & 0 & 2 \\ -1 & 0 & 1 \end{pmatrix} \quad (1)$$

$$K(G_y) = \begin{pmatrix} 1 & 2 & 1 \\ 0 & 0 & 0 \\ -1 & -2 & -1 \end{pmatrix} \quad (2)$$

Then the gradient magnitude is calculated as the Euclidean distance:

$$|G| = \sqrt{G_x^2 + G_y^2} \quad (3)$$

Because the margins are sometimes expanded, they cannot be correctly defined. The edge direction must be determined in order to solve this issue using:

$$\theta = arctan\ \frac{|G_x|}{G_y} \quad (4)$$

The fuzzy edges are sharpened as a result of this. All other points are rejected while local maxima are kept. The following technique is followed for each pixel:

- Using the 8 closest neighbours, gradient directions are rounded off nearing 45^o.
- Comparing current pixel edge strengths in both positive and negative directions of gradients along with comparisons of pixels in the north and south when pixel directions are north, i.e. 90.
- Highest values for edges of current pixels are maintained while other values are suppressed.

The intensity of the retained pixels is used to identify them. Many of these pixels are points of genuine edges, but others are formed by noise or colour fluctuation. For identifying and deleting erroneous edge pixels, dual thresholds namely greatest and lowest are used by Canny edge detections as stronger pixels have larger values than upper thresholds while weaker pixels have values lesser than lower thresholds. Weak edges connected to strong edges are not discarded. Strong edges are considered important and directly included in final outputs.

Classifying ADs using DCCAEs (Deep Clustering and CAEs)

CAEs in general have layers which correspond to encoders $f_W(.)$ and decoders $g_U(.)$. They seek codes for input samples by minimizing MSEs (mean squared errors) between inputs and outputs in over all samples, i.e.

$$\min_{w,u} \frac{1}{n} \sum_{i=1}^{n} \left\| gu\left(f_W(x_i)\right) - x_i \right\|_2^2 \quad (5)$$

Where x and h are vectors, and is a sigmoid activation function similar to ReLU. For the purpose of clarity, the prejudice has been removed. Following training, the embedded code h serve as new representations of input samples. SAEs (Stacked Auto Encoders) are formed by feeding h into another auto encoder. CAEs are used to utilise the spatial structure of pictures.

$$f_w(x) = \sigma(x * w) \equiv h \quad (6)$$
$$g_{u(h)} \equiv \sigma(h * U) \quad (7)$$

Where x and h are matrices or tensors, and "*" is convolution operator. The SCAEs (Stacked CAEs) can be constructed in a similar way as SAEs.

The proposed CAEs do not require time-consuming layer-by-layer pre-training. To extract hierarchical features, various convolution layers are placed on the input pictures first. Then, in the last convolution layer, flatten all units to produce a vector, followed by an embedded layer, which is a completely linked layer with just 10 units. As a result, the original 2D picture is converted into a 10-dimensional feature space. For unsupervised training, fully linked layers and many convolution transpose layers are employed to send embedded information back to original images. The encoder parameters h $=F_w(x)$ and decoder x' = $G_{\omega'}(h)$ are updated by minimizing the reconstruction error:

$$L_r = \frac{1}{n} \sum_{i=1}^{n} \left\| G_{\omega'}\left(F_{\omega}(x_i)\right) - x_i \right\|_2^2 \quad (8)$$

Where n is the number of images in dataset,$x_i \in R^2$ is the ith image.

Key aspect of the proposed CAEs is their aggressive constraints on dimensions of embedded layers. If embedded layers are large enough, networks can repeat inputs to outputs, resulting in learning of irrelevant properties. Keeping the dimension of latent code h lesser than the input data x are an easy way of preventing identity mappings. The auto encoder is forced to capture the most important aspects of the data when learning such incomplete representations. As a result, the size of embedded spaces were limited to counts of dataset clusters as it enables the network to be trained till end without the need for regularisation techniques like Dropouts or Batch Normalizations. The clustering challenge has shown that the trained compact representations are successful. Another difference is that in the encoder, we use a convolution layer with stride instead of a convolution layer followed by a pooling layer, and in the decoder, we use a convolution transpose layer with stride. Because stride convolution (transpose) layers allow the network to learn spacial sub sampling (upsampling) from data, the network's transformation capability increases. Because we are not aiming for cutting-edge clustering performance, we do not use fancy layers or methods like as Batch Normalization, Leaky Re- Lu activation, or layer-wise pretraining. In image clustering tasks, we only show that CAEs outperform fully linked SAEs.

DCEC (Deep Convolution Embedded Clustering)

When compared to fully linked SAE, CAEs are more powerful networks for dealing with pictures. As a result, DEC (Deep Embedded Clustering) is enhanced by using CAEs instead of SAEs. Then we propose that employing solely clustering oriented loss in DEC may corrupt the embedded feature space. To do this, the auto encoder reconstruction loss is introduced to the goal and optimised simultaneously with the clustering loss. The auto encoders will retain the local structure of the data generation distribution, preventing feature space corruption. DCEC (Deep Convolution Embedded Clustering) is the name of the resultant algorithm. The structure of DCEC is described first, followed by a detailed description of the clustering loss and local structure preservation mechanisms. Finally, the optimization method is shown.

Structure of DCEC

DCEC structures are made of CAEs along with clustering layers linked to embedded layers. Clustering layers convert embedded points z_i of input images x_i into soft labels. The clustering loss L_c is defined as Kullback-Leibler divergence (KL divergence) between distributions of soft labels and predefined target distributions. Clustering losses cause embedded features to form clusters, and CAEs are employed to prevent this and learn embedded features. The DCEC's goal is to

$$L = L_r + \gamma L_C \qquad (9)$$

where Lr stands for reconstruction losses, Lc represents clustering losses, and $\gamma > 0$ represents coefficients that control distortion degrees of embedded spaces. When $\gamma = 1$ and $Lr \equiv 0$, (5) reduces to the objective of DEC.

Clustering Layer and Clustering Loss

The clustering layer and loss are directly borrowed from DEC.Briefly review their definitions for completeness of DCEC structure. The clustering layer maintains cluster centers $\{\mu_j\}_1^k$ as trainable weights and maps each embedded point z_i into soft label q_i by Student's t-distribution.

$$q_{ij} = \frac{\left(1+\|z_i-\mu_j\|^2\right)}{\sum_j\left(1+\|z_i-\mu_j\|^2\right)^{-1}}^{-1} \qquad (10)$$

where q_{ij} is the j_{th} entry of q_i, representing the probability of z_i belonging to cluster j. The clustering loss is defined as

$$L_c = KL(P \parallel Q) = \sum_I \sum_J P_{ij} \log \frac{p_{ij}}{q_{ij}} \qquad (11)$$

Where P is the target distribution, defined as

$$p_{ij} = \frac{q_{ij}^2 / \Sigma_i q_{ij}}{\Sigma_j \left(q_{ij}^2 / \Sigma_i \ q_{ij} \right)} \qquad (12)$$

Reconstruction Loss for Local Structure Preservation

DEC discards the decoder and fine-tunes the encoder using clustering losses L_c. Considering how this fine-tuning could distort the embedded space, the representativeness of embedded features are reduced and hence damage clustering performances.

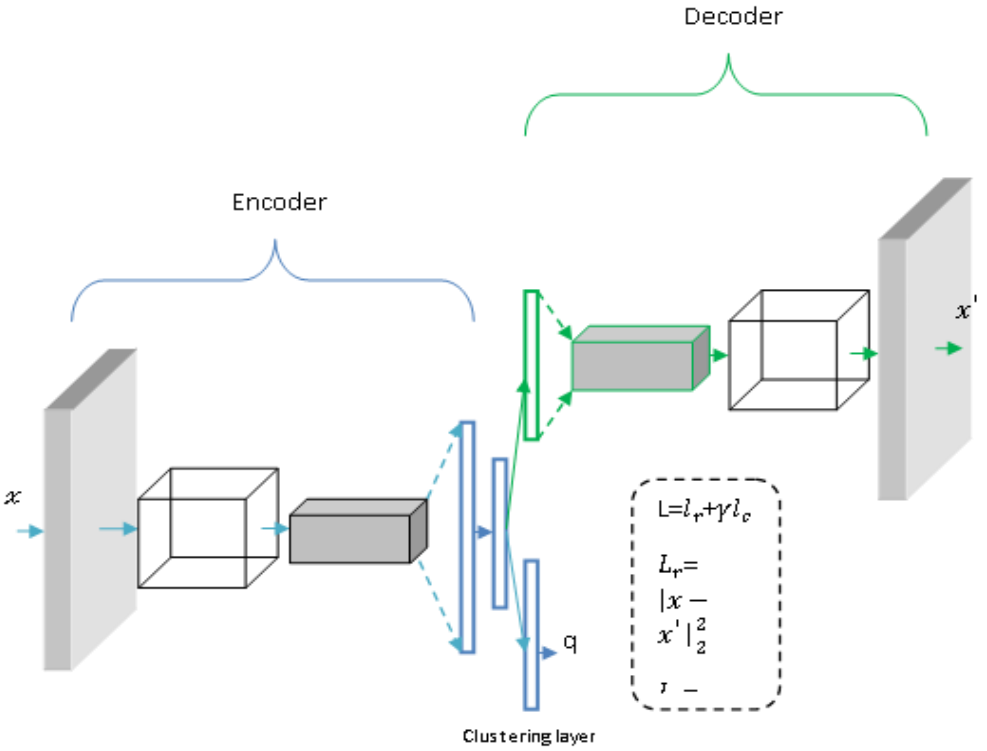

Figure: 2.The structure of deep DCEC

As a result, the decoders are bye passed and clustering losses are added to the embedded layer. Autoencoders can preserve the local structure of the data producing distribution. Softly changing embedded space s- with clustering loss L_c will not result in corruption in this situation. Hence, coeffcient γ is better when < 1, which will be empirically fixed in the range 0:1 for all experiments.

Optimization

To generate a meaningful target distribution, first pretrain the parameters of CAE by setting = 0. The cluster centres are initialised using k-means on embedded characteristics of all photos after prêt-raining. Then set γ = 0:1 and update CAE's weights, cluster centers and target distribution P as follows.

Update weights and cluster centers of CAEs

As $\frac{\vartheta L_c}{\vartheta z_i}$ and $\frac{\vartheta L_c}{\vartheta \mu_j}$are Using back propagation and mini-batch SGD, the weights and centres may be updated Reorganize the target distribution. The intended audience P is the ground truth soft label, although it is also influenced by the expected soft label. To avoid instability, P should not be changed using merely a batch of data at each iteration. In reality, we update the target distribution every T iterations utilising all embedded points. The update rules may be found in sections (6) and (8). If the change in label assignments between two consecutive updates for target distribution is less than a threshold δ, the training procedure ends.

Results and Discussion

This section analyses the results of the experiments carried out on the proposed model. The implementation of this model is carried out with the help of MATLAB. In comparison of the already variable CAE algorithm and the proposed DCEC are done in terms of precision, recall, accuracy, F-measure and error rate.

Table: 1. Performance comparison results

Metrics	Methods	
	CAE	DCEC
Precision (%)	90.5	93
Recall: (%)	84	92
Accuracy (%)	90.5	93.5
F1score (%)	84	90

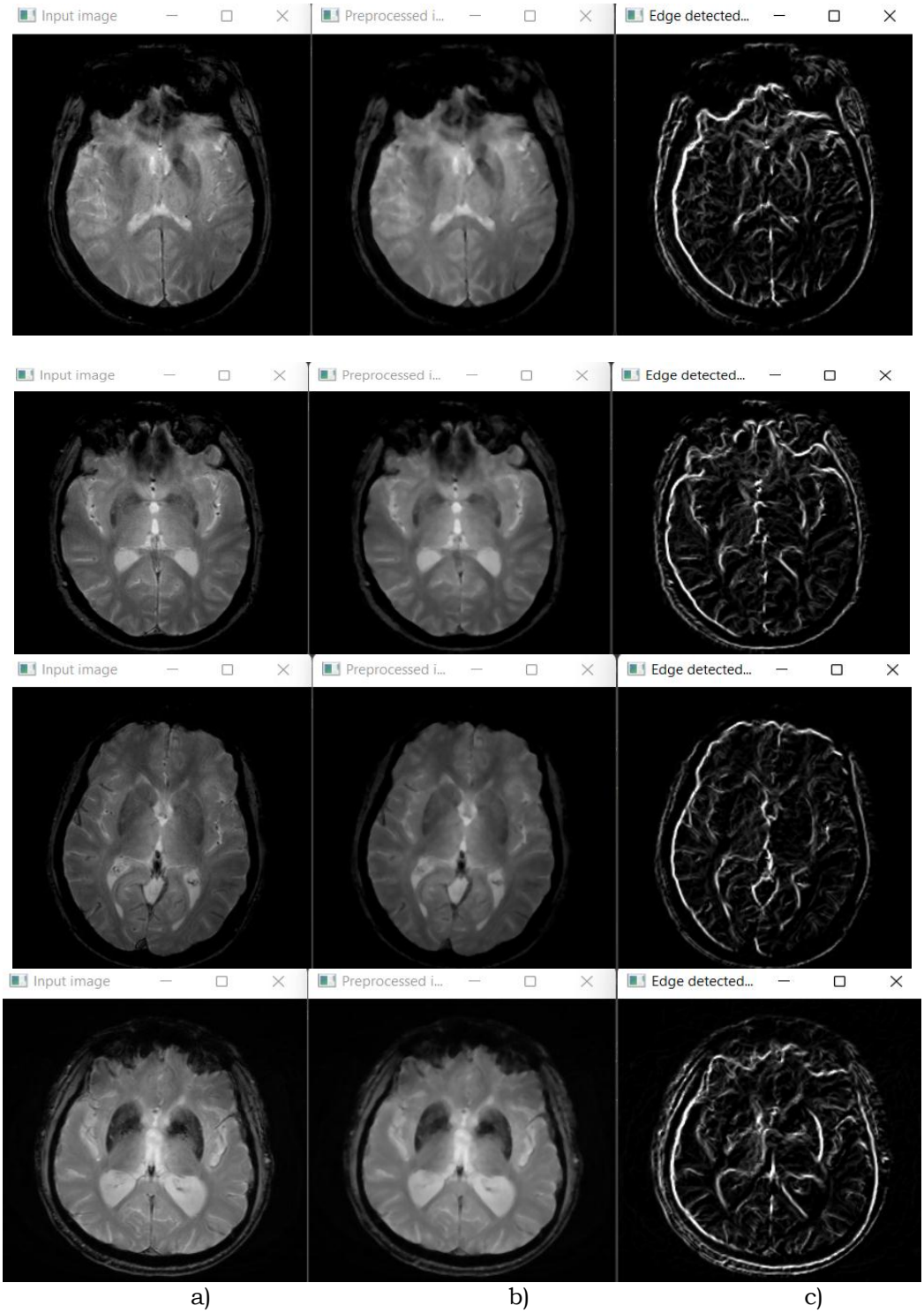

a) b) c)

Figure: 3.a) Input image b) Pre-processed image c) Edge detection images

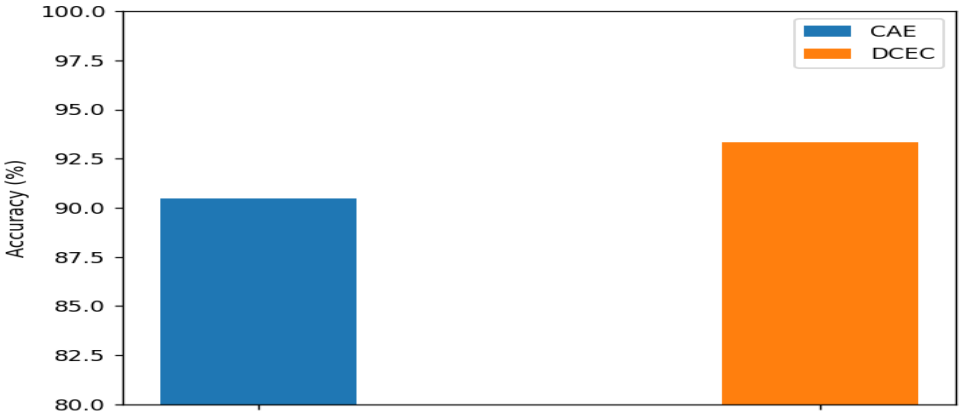

Figure: 4. Accuracy results vs. classification methods

The accompanying chart shows a performance comparison of Accuracy metrics with CAEs suggested DCEC system. The proposed study employs an edge detection approach to increase the DCEC's accuracy. Different approaches are depicted on the X-axis, while accuracy values are represented on the Y-axis. As can be seen from the findings, the newly introduced DCEC model achieved greater accuracy results of 93.5 percent, whereas the existing CAEs produced only 90.5 percent accuracy.

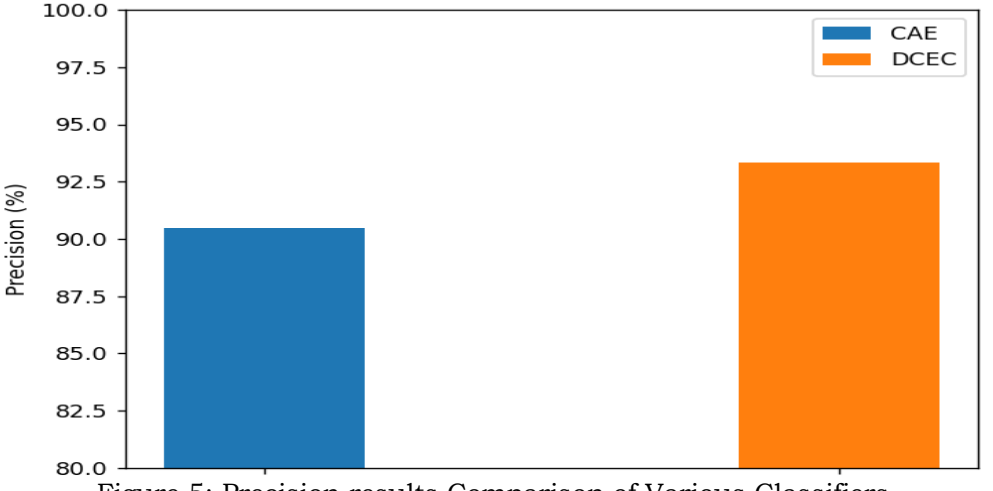

Figure 5: Precision results Comparison of Various Classifiers

The suggested DCEC's efficiency is demonstrated in the above figure by comparing it to existing CAE approaches in terms of accuracy. Noise reduction is used as a pre-processing step in the proposed work, which improves accuracy. Different approaches are displayed in the X-axis, while accuracy values are represented in the Y-axis. As can be seen from the findings, the newly introduced DCEC model provided precision results of 93 percent, whereas existing CAEs only produced 90.5 percent.

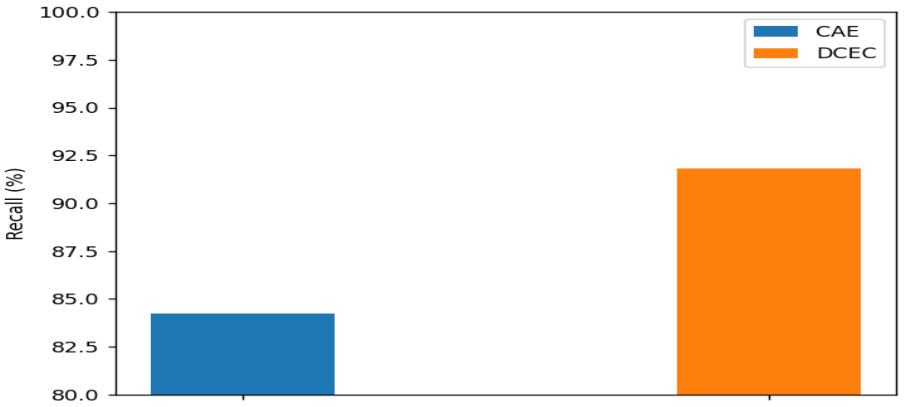

Figure: 6. Recall results vs. classification methods

Figure 6 compares the recall of the present classifier CAE's suggested DCEC scheme to that of the existing classifier. Clustering in CNNs BY is used in the proposed study, which boosts the recall rate. The X-axis in the graph above represents different approaches, while the Y-axis represents recall levels. As can be seen from the data, the newly introduced DCEC model has a greater recall rate of 92 percent, whereas the existing CAEs only have an 84 percent recall rate.

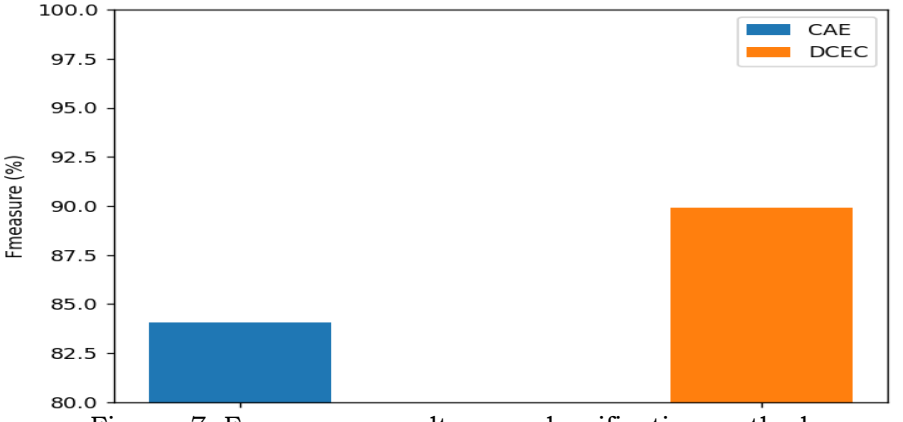

Figure: 7. F-measure results vs. classification methods

The performance comparison for F-measure metrics with the classifiers CAEs suggested DCEC methods is shown in the graph above. Different approaches are depicted on the X-axis, while F-measure values are represented on the Y-axis. As can be seen from the findings, the newly introduced DCEC model provided f-measure values of 90% whereas CAEs only produced 84 percent.

Conclusion and Future Work

ADs are chronic neurodegenerative disease where early diagnosis assists in considerably reducing risks of further deteriorations. This work modelled automated classifications of ADs. T5he model uses a median filtering based pre-processing to remove the unwanted noise in the image. Edge detection is

proposed using canny edge detection operator. Finally the image is fed into the Deep Clustering with CAEs for classifying ADs and NCs. Experimental results show that this proposed model provides better results in terms of precisions, recalls, accuracies and f-measures. This work does not implemented for other brain related diseases diagnosis and this could be considered in future work.

References

1. Li, W., Zhao, Y., Chen, X., Xiao, Y. and Qin, Y., 2018. Detecting Alzheimer's disease on small dataset: A knowledge transfer perspective. IEEE journal of biomedical and health informatics, 23(3), pp.1234-1242.
2. Xu, L., Yao, Z., Li, J., Lv, C., Zhang, H. and Hu, B., 2019. Sparse feature learning with label information for Alzheimer's disease classification based on magnetic resonance imaging. IEEE Access, 7, pp.26157-26167.
3. Sarraf, S. and Tofighi, G., 2016, December. Deep learning-based pipeline to recognize Alzheimer's disease using fMRI data. In 2016 future technologies conference (FTC) (pp. 816-820). IEEE.
4. Shakarami, A., Tarrah, H. and Mahdavi-Hormat, A., 2020. A CAD system for diagnosing Alzheimer's disease using 2D slices and an improved AlexNet-SVM method. Optik, 212, p.164237.
5. Amin-Naji, M., Mahdavinataj, H. and Aghagolzadeh, A., 2019, March. Alzheimer's disease diagnosis from structural MRI using Siamese convolution neural network. In 2019 4th International Conference on Pattern Recognition and Image Analysis (IPRIA) (pp. 75-79). IEEE.
6. Zhang, J., Liu, M., An, L., Gao, Y. and Shen, D., 2017. Alzheimer's disease diagnosis using landmark-based features from longitudinal structural MR images. IEEE journal of biomedical and health informatics, 21(6), pp.1607-1616.
7. Li, F., Cheng, D. and Liu, M., 2017, October. Alzheimer's disease classification based on combination of multi-model convolution networks. In 2017 IEEE international conference on imaging systems and techniques (IST) (pp. 1-5). IEEE.
8. Billones, C.D., Demetria, O.J.L.D., Hostallero, D.E.D. and Naval, P.C., 2016, November. DemNet: a convolution neural network for the detection of Alzheimer's disease and mild cognitive impairment. In 2016 IEEE region 10 conference (TENCON) (pp. 3724-3727). IEEE.
9. Wang, Y., Yang, Y., Guo, X., Ye, C., Gao, N., Fang, Y. and Ma, H.T., 2018, July. A novel multimodal MRI analysis for Alzheimer's disease based on convolution neural network. In 2018 40th Annual International Conference of the IEEE Engineering in Medicine and Biology Society (EMBC) (pp. 754-757). IEEE.
10. Feng, C., Elazab, A., Yang, P., Wang, T., Zhou, F., Hu, H., Xiao, X. and Lei, B., 2019. Deep learning framework for Alzheimer's disease diagnosis via 3D-CNN and FSBi-LSTM. IEEE Access, 7, pp.63605-63618.
11. Hosseini-Asl, E., Keynton, R. and El-Baz, A., 2016, September. Alzheimer's disease diagnostics by adaptation of 3D convolution network. In 2016 IEEE international conference on image processing (ICIP) (pp. 126-130). IEEE.
12. Manzak, D., Çetinel, G. and Manzak, A., 2019, August. Automated Classification of Alzheimer's disease using deep neural network (DNN) by

random forest feature elimination. In 2019 14th International Conference on Computer Science & Education (ICCSE) (pp. 1050-1053). IEEE.
13. Aranda, L.A., Reviriego, P. and Maestro, J.A., 2017. Error detection technique for a median filter. IEEE Transactions on Nuclear Science, 64(8), pp.2219-2226.
14. Meher, S.K. and Singhawat, B., 2014. An improved recursive and adaptive median filter for high density impulse noise. AEU-International Journal of Electronics and Communications, 68(12), pp.1173-1179.
15. Gupta, V., Chaurasia, V. and Shandilya, M., 2015. Random-valued impulse noise removal using adaptive dual threshold median filter. Journal of visual communication and image representation, 26, pp.296-304.
16. Xu, Q., Varadarajan, S., Chakrabarti, C. and Karam, L.J., 2014. A distributed canny edge detector: algorithm and FPGA implementation. IEEE Transactions on Image Processing, 23(7), pp.2944-2960.
17. Nikolic, M., Tuba, E. and Tuba, M., 2016, November. Edge detection in medical ultrasound images using adjusted Canny edge detection algorithm. In 2016 24th Telecommunications Forum (TELFOR) (pp. 1-4). IEEE.
18. Yuan, L. and Xu, X., 2015, August. Adaptive image edge detection algorithm based on canny operator. In 2015 4th International Conference on Advanced Information Technology and Sensor Application (AITS) (pp. 28-31). IEEE.
19. Wang, Z., Li, M., Wang, H., Jiang, H., Yao, Y., Zhang, H. and Xin, J., 2019. Breast cancer detection using extreme learning machine based on feature fusion with CNN deep features. IEEE Access, 7, pp.105146-105158.
20. Alkhaleefah, M. and Wu, C.C., 2018, October. A hybrid CNN and RBF-based SVM approach for breast cancer classification in mammograms. In 2018 IEEE International Conference on Systems, Man, and Cybernetics (SMC) (pp. 894-899). IEEE.